JJEE
Volume 5, Number 1, 2019
Pages 61-76
Jordan Journal of Electrical Engineering
ISSN (Print): 2409-9600, ISSN (Online): 2409-9619

A Novel Flexible Cloud Shape Loop Antenna for Muscle Implantable Devices

Rula S. Alrawashdeh[a], Fatima H. Alharazneh, Sarah A. Alsarayreh, Enas S. Aladaileh

Department of Electrical Engineering, Mutah University, Al-Karak, Jordan
[a]e-mail: rularsr18@gmail.com

Received: December 4, 2018 *Accepted: February 23, 2019*

Abstract— In this paper, a novel flexible cloud shape loop antenna is designed and proposed for implantable applications at the Medical Device Radiocommunications Service (MedRadio 401-406 MHz) and Industrial, Scientific and Medical (ISM 433-434 MHz and 2.4-2.5 GHz) bands. The antenna has a small size; and it can be bent around small cylindrical implants that are 3.7 mm in radius and 10.6 mm in length. It is formed in the shape of a cloud to increase antenna radiation efficiency and gain by increasing its radiation resistance and near magnetic field in comparison with that for a typical elliptic cylindrical loop antenna. The radiation efficiency and gain of the proposed antenna are increased by 2.4 dB and 2.5 dBi, respectively, at 403 MHz in comparison with that for the elliptic cylindrical loop antenna. The antenna is also simulated in an anatomical arm model. The proposed antenna has many attractive features (small size, light weight and relatively good radiation efficiency and gain); and hence it could be a good candidate for implantable applications.

Keywords— Implantable antenna, ISM band, Loop antenna, MedRadio.

I. INTRODUCTION

There has been an increasing interest in Bio-telemetric healthcare applications such as glucose monitoring. In a typical bio-telemetric health care system, the data are transmitted wirelessly from a transmitter inside the human body to an external receiver outside of it [1]. The implantable antenna plays the main role in transferring data wirelessly in such a system. However, the design of such an antenna is very challenging. This antenna works in the lossy and non-uniform human body which absorbs most of the implantable antenna radiation [1], [2]. Hence, a small portion of the power is only radiated out of the human body. Also, the performance of the implantable antenna may be altered in the real human body. This requires: a broad bandwidth in order to guarantee a deep matching (S11< -10 dB) if detuning happens in the real human body, miniaturization as the antenna is required to work at the 401-406 MHz Medical Device Radio communications Service (MedRadio) band [3] over a small size (in the range of hundreds of mm^3), and satisfaction of the biocompatibility and Specific Absorption Rate (SAR) requirements. The SAR is required to be smaller than 1.6 W/kg when it is taken over the volume containing a mass of 1 gram of the absorbing tissue (1-g avg SAR<1.6 W/kg) [4] or smaller than 2 W/kg for a volume containing 10 gram of the absorbing tissue (10-g avg SAR<2 W/kg) [5]. The antenna is also preferred to work for other bands such as the 433 MHz and 2.45 GHz Industrial, Scientific and Medical (ISM) bands to support the functionalities of wireless power transfer and power saving [1], [6]. Hence, it is very challenging to satisfy all of these requirements at the same time. Many antennas of different structures and types were proposed in literature for implantable applications. In [7]-[10], patch antennas were proposed for implantable applications at 2.45 GHz. The human body losses at this frequency are larger than that at 403 MHz. In [11] patch antennas were also proposed but at 403 MHz. The problem related with patch antennas, which are electric in type is that they are rigid and, hence, are usually placed inside the implant. This leaves a small

Corresponding author's e-mail: rularsr18@gmail.com

space for other components inside the implant as the antenna exploits a large internal space. Moreover, implantable patch antennas are usually narrow in bandwidth [11]. Magnetic type antennas such as loop and slot antennas have been found to outperform electrical type antennas in the nonmagnetic human body which does not present magnetic losses [11]. In [12], a slot antenna was also proposed. Loop antennas were also designed in [13]. However, these antennas were rigid in structure. Flexible antennas are lighter in weight; and they provide better utilization of the implant structure than rigid type antennas [1]. Some flexible antennas were proposed in [14]-[19]. However, these antennas were either large in size or did work for only one or two of the frequency bands that are required for implantable applications. Some antennas like in [6] were difficult to manufacture, so they caused discrepancies between simulations and measurements. Moreover, antennas of typical basic structures are found to provide a moderate performance. Therefore, it is required to exploit the antenna structure effectively in order to optimize its performance [20], [21]. Hence, small flexible antennas, which work for all of the 401-406 MHz, 433-434 MHz and 2.45-2.4835 GHz ISM bands of a robust performance, are still needed. These antennas are required to exploit the structure in a good way that keeps the antenna simple and improves all of its radiation characteristics. In this paper, a small flexible cloud shape loop antenna is proposed to work for the 401-406 MHz MedRadio, 433 MHz and 2.45 GHz ISM bands. The antenna structure is optimized to form a cloud shape in order to enclose a larger magnetic near field in comparison with that of a typical elliptic cylindrical loop antenna. This is reflected on increasing the antenna gain and radiated power.

This paper is arranged as the following: In Section II, the antenna structure and design parameters are presented and compared with those of a typical elliptic cylindrical loop antenna. In Section III, the antenna performance is evaluated and analyzed at the three bands of interest in a simplified body model. Then, the performance is evaluated in the arm of the Simulation package CST Microwave Studio Katja voxel body model in Section IV. Finally, the paper is concluded in Section V.

II. ANTENNA STRUCTURE

The proposed antenna is shown in Fig. 1. The antenna is of a cloud shape. It has outer dimensions of 22.9 and 10.6 mm. This antenna is flexible, so it can be bent around the outer or inner wall of a cylindrical implantable device that is 3.7 mm in radius and 10.6 mm in length. This is 26% smaller in radius and 29.3% shorter in length than the cylindrical implant around which the antenna in [6] can be bent. Such an antenna can be used with implants for children or in body areas of thin muscle layers.

The modification is intended to obtain the following:

1. Increase the antenna radiation resistance and hence the antenna radiation efficiency: The antenna radiation resistance R_r (Ω) of a simple loop antenna is given as (1) [22]:

$$R_r = 20\pi^2(\frac{C}{\lambda_0})^4 \quad (1)$$

Where C (m) is the circumference of the loop; and λ_0 (m) is the free space wavelength.

This radiation resistance increases with the circumference (C).

The antenna radiation efficiency (η) increases when the radiation resistance is increased [22]:

$$\eta = \frac{R_r}{R_r+R_L} \quad (2)$$

where R_L (Ω) is the loss resistance of the antenna.

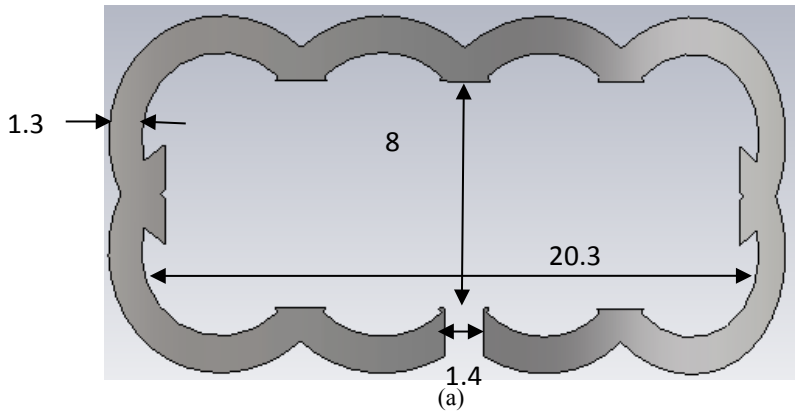

(a)

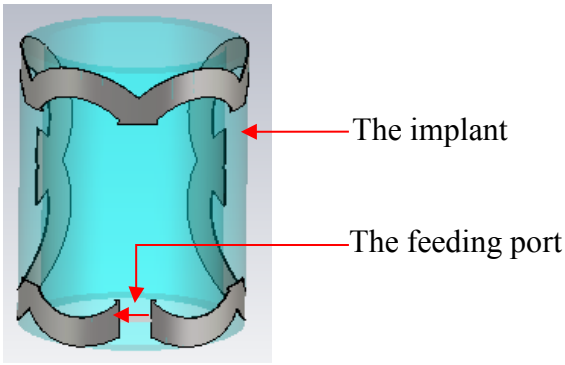

(b)

Fig. 1. The proposed cloud shape loop antenna: a) flat, and b) bent structures (unit: mm)

The antenna is modified from a typical elliptic cylindrical loop antenna that is shown in Fig. 2.

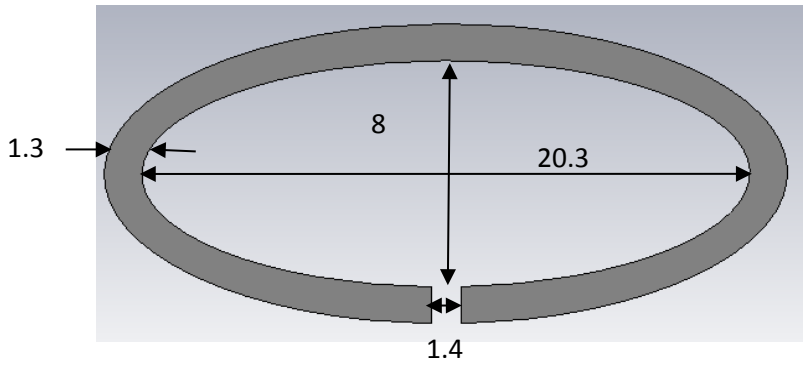

(a)

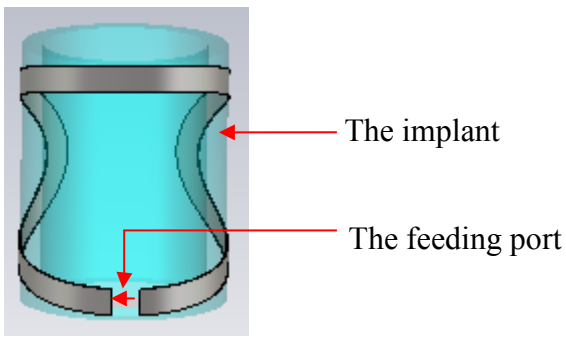

(b)

Fig. 2. A typical elliptic cylindrical loop antenna: a) flat, and b) bent structures (unit: mm)

The radiation resistance and the radiation efficiency are increased for the proposed antenna by introducing round loops to the typical elliptic cylindrical loop antenna structure. These round loops help increase the antenna circumference and hence the antenna radiation resistance and efficiency. The circumference of the cloud shape loop antenna is 45% larger than that of the typical elliptic cylindrical loop antenna while the same outer antenna dimensions are kept.

2. Increase the antenna gain: Unlike antennas in free space, the gain of the implantable antenna in the lossy human body (G_{con}) increases with the near magnetic field $|H|$ (A/m) (3) [23].

$$G_{con} = \frac{4\pi \sqrt{(\omega\mu/2\sigma)}\,(|H|de^{(d/\delta)})^2}{R_r(i_i)^2} \tag{3}$$

where d (m) is the distance at which $|H|$ is taken or measured; δ (m) is the skin depth; R_r (Ω) is the radiation resistance; i_i (A) is the input current; ω (rad/m) is the angular frequency; μ (H/m) is the permeability which is equal to μ_0 for the nonmagnetic human body; and σ (S/m) is the conductivity of the human body tissue.

Electromagnetic fields of the antenna are classified into near and far fields based on their proximity to the antenna as shown in Fig. 3 [22]. The near magnetic field for the antenna proposed in this paper is taken at a very close proximity to the antenna at its surface and at short distances inside the human body. The far fields are taken at a distance of 2.5 m, which is longer than $3\lambda_0$ at 403 MHz.

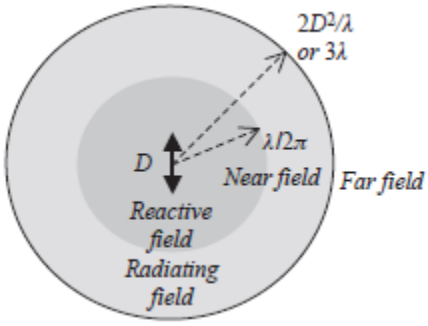

Fig. 3. The field regions of an antenna of a maximum dimension of D [22]

The near magnetic field is increased for the antenna proposed in this paper. The round loops in the cloud shape structure are confining a larger magnetic field than that of the typical elliptic cylindrical loop antenna as shown in the following section.

III. PERFORMANCE AND ANALYSIS

A) Performance at the (401-406) MHz MedRadio and 433 MHz ISM Bands

The cloud shape loop antenna is simulated at the center of a simplified body model as shown in Fig. 4. This body model has the following characteristics:

- A single layer that mimics the dielectric properties of a human muscle at 403 MHz (ε_r= 57.1 and σ= 0.797 S/m [24]).
- A cylindrical shape which is 100 mm in diameter and 50 mm in height.

Simulations are conducted via the Simulation package CST Microwave Studio [25]. Hexahedral meshes are employed; and a minimum distance of λ/4 is kept between the structure and the edge of the simulation space. The antennas are fed by discrete ports of 50 Ω with an input power of 1 W.

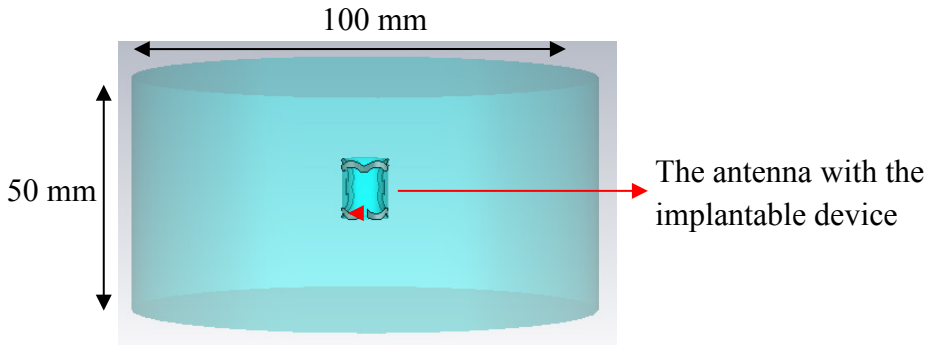

Fig. 4. The simplified cylindrical body model of simulations in this paper

The simulated reflection coefficient is shown in Fig. 5. The antenna has a broad -10 dB bandwidth covering both of the (401-406 MHz) MedRadio and 433 MHz ISM bands. The dielectric properties of the human muscle tissue are ε_r= 56.87 and σ=0.8 at 433 MHz [24]; and they are very close to the corresponding dielectric properties at 403 MHz. Therefore, the same reflection coefficient S_{11} is obtained at both of the 403 and 433 MHz bands.

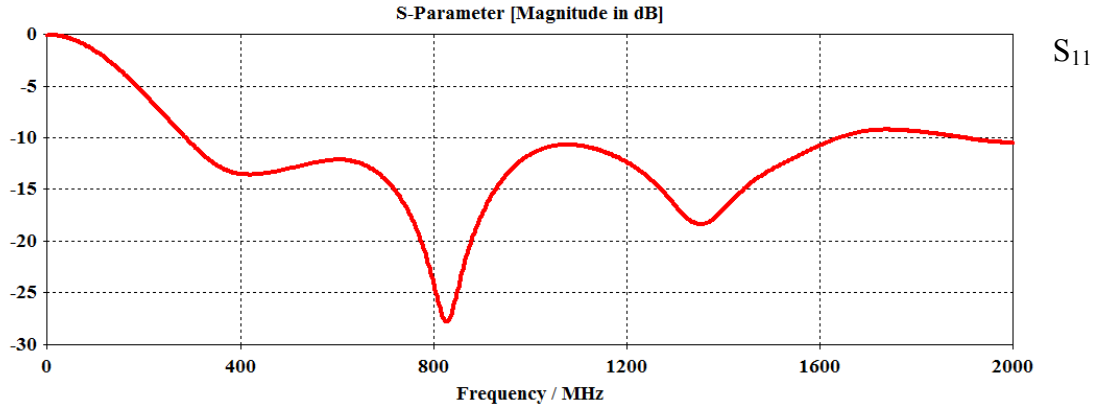

Fig. 5. The simulated reflection coefficient S11 (dB) of the proposed cloud shape loop antenna in the simplified body model

The simulated 3D and polar gain patterns at 403 and 433 MHz are shown in Fig. 6. The antenna has an intended maximum radiation in an off body direction at θ=42 degrees at both of these frequencies. The antenna has obtained maximum realized gain values of -31.5 and -29.2 dBi at 403 and 433 MHz, respectively. The total radiation efficiencies are 0.024 and 0.043% at 403 and 433 MHz, respectively. Larger radiation efficiencies and gain are obtained at 433 MHz than at 403 MHz in correspondence with the results in [1]. The antenna is electrically larger at this frequency than that at 403 MHz. The small realized gain and radiation efficiency at both bands are mainly attributed to the human body losses.

The surface current of the proposed antenna at 403 MHz and 433 MHz is shown in Fig. 7. Strong current densities are noticed at the side round loops. The same distribution is almost obtained at 403 MHz and 433 MHz.

It is worth indicating that the antenna resonates at f_0 =3.62 GHz in free space. It also obtains a radiation efficiency of -0.4 dB (91.2%) and realized gain of 1.34 dBi. The resonant frequency is shifted down from (f_0) to (f_r) inside the human body as $f_r = f_0/\sqrt{\varepsilon_r}$. The radiation efficiency and gain are decreased inside the human body because of its losses.

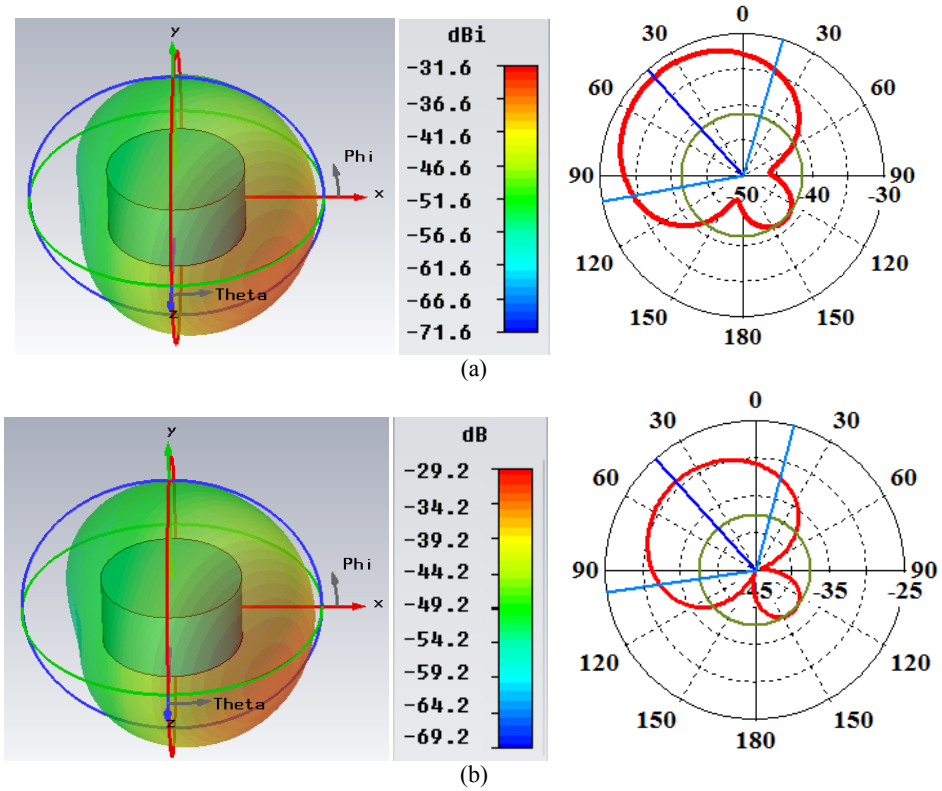

(a)

(b)

Fig. 6. The simulated 3D and polar at (Φ= 0 and θ= 42 degrees) realized gain patterns of the proposed antenna at: a) 403 MHz, and b) 433 MHz

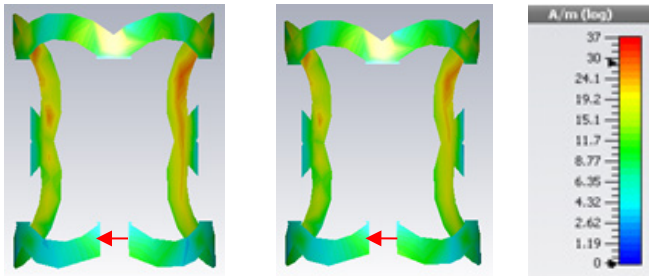

(a) (b)

Fig. 7. The surface current at: a) 403 MHz, and b) 433 MHz

As the antenna will be placed inside the human body, it should be biocompatible. As stated above, the antenna can be bent around the inner wall of the implant, which is normally manufactured from a biocompatible material such as Poly-ether-ether-ketone (PEEK) [11]. Hence, the implant wall serves as the insulation layer between the conducting radiator and the surrounding human body tissues. The implantable device in this work is simulated with the dielectric properties of PEEK ($\varepsilon'_e - j\varepsilon''_e = 3.2 - j\,0.032,\ tan\delta = 0.01$) [11]. The proposed antenna can be also bent around the outer wall of the implant; and a biocompatible insulation layer of PEEK can be placed on the top of it. When the thickness of this layer is increased, the antenna matching at the intended bands of operation may be altered. The radiation efficiency and gain may increase for this case as the lossy area around the antenna is decreased. To evaluate the effect of the insulation layer thickness on the performance of the proposed antenna, simulations with a PEEK layer of different thicknesses are conducted. The simulation results show that an insulation PEEK layer of up to 0.25 mm thickness can be placed around the antenna while keeping a good matching (S_{11}< -10 dB) and maintaining the same radiation properties.

The antenna should also comply with the SAR specifications. The SAR is a measure of the power absorbed by the human body tissues surrounding the antenna. It can be defined as (4) [26]:

$$\mathrm{SAR} = \frac{\sigma|\mathrm{E}|^2}{2\rho} \tag{4}$$

Where $|E|$ (V/m) is the peak value of the near electric field intensity; and ρ (kg/m^3) is the tissue mass density. The mass density for muscle is 1040 kg/m^3 [1].
The maximum root mean square (rms) value of the SAR, which averaged over 1 gram of the absorbing tissue (1-g avg SAR), is computed at 403 MHz and 433 MHz frequencies with an input rms power of 0.5 W. The 1-g avg SAR limitations are much more restricted than the 10-g avg SAR. The results are provided in Table 1.

TABLE 1
MAXIMUM RMS 1-G AVG SAR (W/KG) AT 403 MHZ AND 433 MHZ.

	403 MHz	433 MHz
Maximum SAR (rms,1g)	224.596	210.713

This means that the antenna can be provided with an input power of up to 3.56 mW to satisfy the 1-g avg SAR specification. This value is larger than 1 mW, which is normally provided to implantable antennas [1], [27]. The maximum SAR for 1-g averaging at 403 MHz when the antenna is provided with an input power of 1 mW, is 0.474 W/kg which is much smaller than 1.6 W/kg. Smaller SAR values are obtained at 433 MHz than at 403 MHz.

B) Performance at the 2.45 GHz ISM Band

The antenna is also simulated in a simplified body model that mimics the dielectric properties of a human muscle at 2.45 GHz (ε_r= 52.7 and σ= 1.74 S/m [24]). The simulated reflection coefficient S_{11} is shown in Fig. 8. It can be seen from the figure that a good matching (S_{11}< -10 dB) has been obtained at 2.45 GHz.

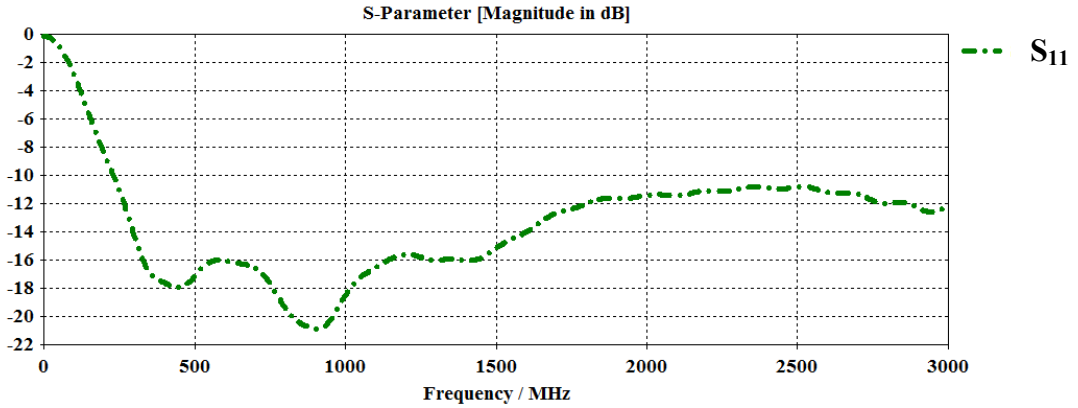

Fig. 8. The reflection coefficient S11 (dB) of the proposed antenna at 2.45 GHz

The antenna radiation pattern is shown in Fig. 9. The antenna has obtained a maximum radiation at the plane Φ= 45 degrees and θ= 131 degrees. The maximum 3D realized gain is -26.3 dBi. The antenna has also obtained good realized gain values at Φ=0 plane and at the angles for which the maximum radiation is obtained at 403 MHz and 433 MHz:

- A realized gain of -27.7 dB at Φ= 0 and θ= 141 degrees.
- A realized gain of -28.86 dBi at Φ= 0 and θ= 42 degrees.

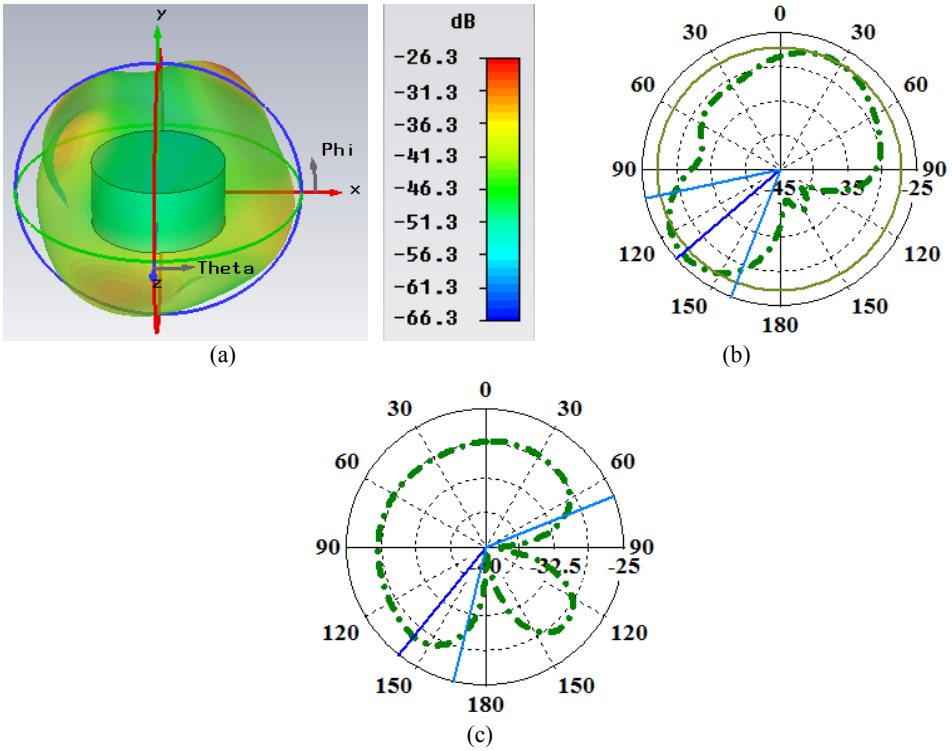

Fig. 9. a) 3D, b) polar at Φ= 45 degrees and θ= 131 degrees, and c) polar at Φ= 0 degrees and θ= 141 degrees realized gain pattern of the proposed antenna at 2.45 GHz

The surface current at 2.45 GHz is shown in Fig. 10. The surface current at the side round loops becomes weaker than that at the rounds in close proximity to the feed.

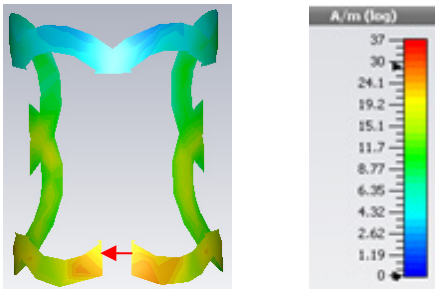

Fig. 10. The surface current at 2.45 GHz

The results show that the proposed antenna can work for the 2.4-2.5 GHz ISM band. Practical implantable chips such as the ZL70101 provided by Microsemi semiconductors are supported by a wakeup receiver. A signal received in the 2.45 GHz ISM band wakes up the IC chip from its sleeping state; subsequently bidirectional communication occurs in the MedRadio (401-406 MHz) spectrum. This capability reduces power consumption so as to extend the lifetime of the implantable device [11].

The maximum rms SAR, which averaged over 1 gram, is 201 W/kg. The SAR decreases with the frequency in correspondence with the results in [1].

C) Comparison with a Typical Elliptic Cylindrical Loop

The cloud shape loop antenna proposed in this paper has shown a relatively large radiation efficiency and gain especially for its small size. This is attributed to its structure that is utilized to increase the antenna radiation efficiency and gain. It is worth indicating that the comparison made between the proposed antenna performance and that of other implantable antennas is inaccurate unless it is conducted in the same body model. However, the

cylindrical body model tends to underestimate the radiation efficiency and gain value [1]. Thus, it is selected for the analysis in this section. The proposed antenna is also evaluated in an anatomical body model in the following section for more accurate results.

The simulated reflection coefficient of the proposed antenna in comparison with that of the typical elliptic cylindrical loop antenna is shown in Fig. 11. It can be seen from the figure that a deeper matching (S_{11}< -10 dB) has been obtained at 403 MHz when the typical elliptic cylindrical loop antenna structure is modified to form a cloud shape. The cloud shape antenna has worked to reduce the resistance of the elliptic cylindrical loop antenna from around 90 Ohms to around 50 Ohms. It has also cancelled out its capacitive reactance by adding a larger inductive reactance.

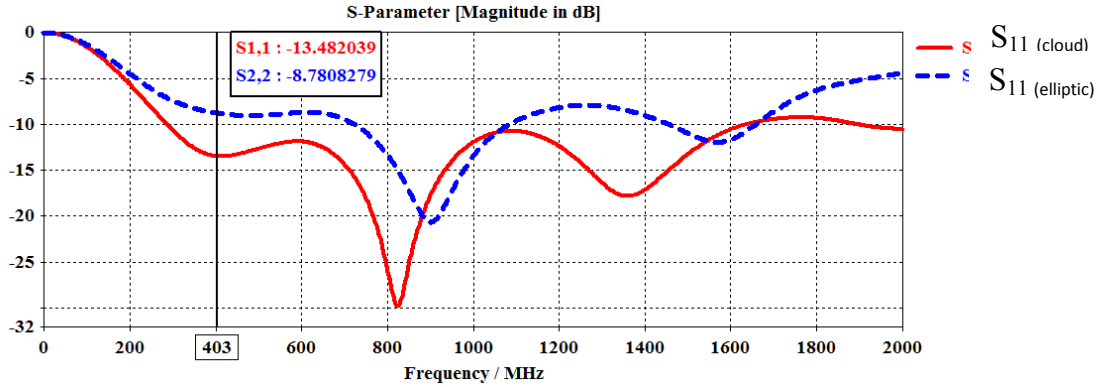

Fig. 11. The reflection coefficient S11 (dB) of the cloud shape and typical elliptic cylindrical loop antennas at 403 MHz

The polar realized gain pattern of the elliptic cylindrical loop antenna is simulated at the azimuth plane and compared to that of the cloud shape loop antenna. The results are shown in Fig. 12. It can be seen from the figure that around 2.5 dBi larger realized gain is obtained for the cloud shape loop antenna at 403 MHz. The maximum radiation is obtained at the off-body direction for both antennas. However, it has been directed 41 degrees clockwise for the elliptic cylindrical loop antenna in comparison with that of the cloud shape loop.

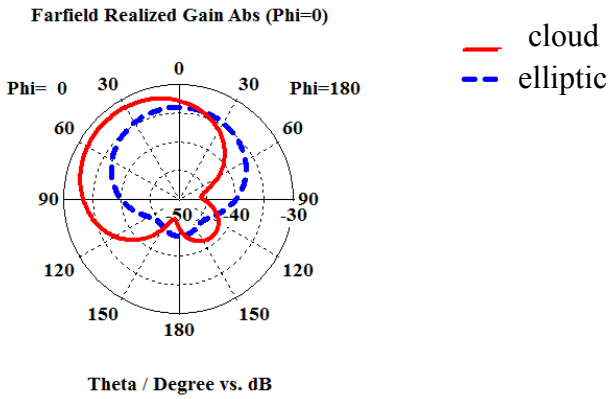

Fig. 12. The polar realized gain pattern of the typical elliptic cylindrical and cloud shape loop antennas at 403 MHz

This has been obtained because the near magnetic field is increased for the cloud shape loop antenna in comparison with that for the typical elliptic cylindrical loop antenna as shown in Fig. 13. The antenna radiation efficiency is also increased by 2.4 dB at 403 MHz.

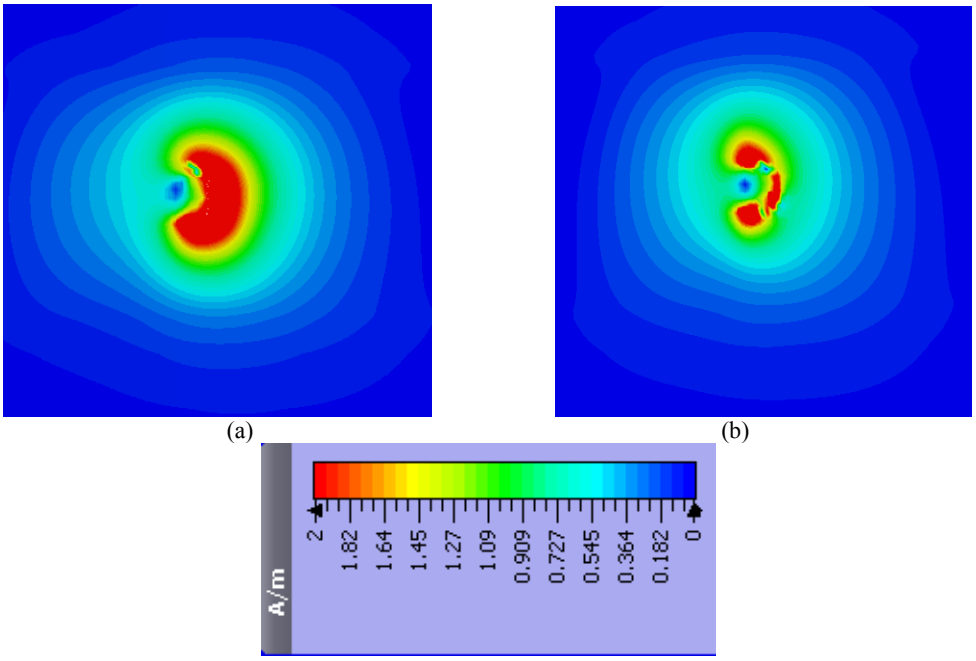

Fig. 13. The magnetic near field intensity of the: a) cloud shape and b) elliptic cylindrical loop antennas

The same improvement in the near magnetic field and gain at 403 MHz is obtained at 433 MHz. The antenna matching (S_{11}< -10 dB) is modified at 2.45 GHz when the antenna is formed in the shape of a cloud as shown in Fig. 14. However, no improvement in the near magnetic field is obtained. The realized gain is increased by 1.34 dBi at 2.45 GHz due to the improvement in the antenna matching. The total radiation efficiency is increased by 2 dB at 2.45 GHz.

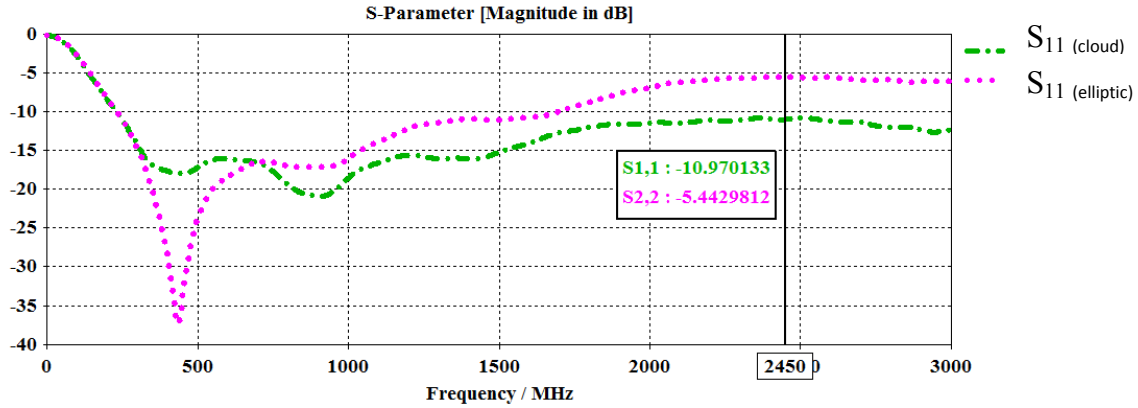

Fig. 14. The reflection coefficient S11 (dB) of the cloud shape and typical elliptic cylindrical loop antennas at 2.45 GHz

The surface current for both of the cloud and elliptic cylindrical loop antennas at 403 MHz and 2.45 GHz are shown in Figs. 15 and 16, respectively. The figures show that the surface current at 403 MHz increases at the round loops that have been introduced to the cloud loop structure. No significant improvement of the surface current at these loops is obtained at 2.45 GHz as it is increased at some parts of the round loops while it is decreased at other parts of them.

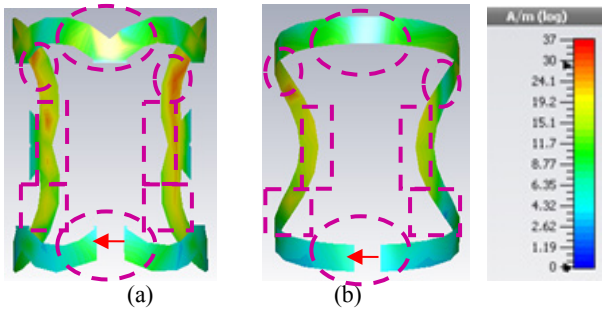

(a) (b)

Fig. 15. The surface current of the: a) cloud and b) elliptic cylindrical loop antennas at 403 MHz

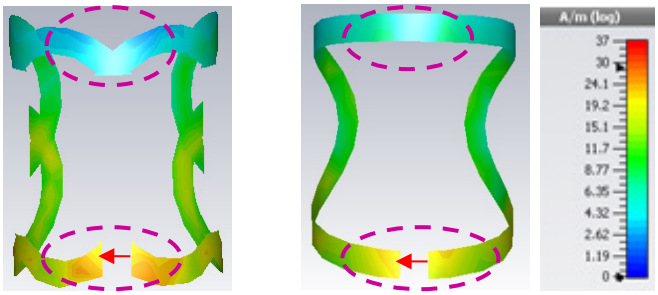

(a) (b)

Fig. 16. The surface current of the: a) cloud and b) elliptic cylindrical loop antennas at 2.45 GHz

A summary of the main characteristics of both of the cloud and elliptic cylindrical loop antennas is provided in Table 2. The 1-g avg SAR has been decreased for the cloud loop antenna in comparison with that for the elliptic cylindrical loop antenna at all of the frequencies of interest as shown in the table.

TABLE 2
SUMMARY OF THE MAIN CHARACTERISTICS OF THE CLOUD AND TYPICAL ELLIPTIC CYLINDRICAL LOOP ANTENNAS

	The Cloud Loop Antenna		The Elliptic Cylindrical Loop Antenna	
The radiation efficiency (%)	403 MHz	0.024	403 MHz	0.0138
	433 MHz	0.043	433 MHz	0.02475
	2.45 GHz	0.096	2.45 GHz	0.06
The maximum 3D realized gain (dBi)	403 MHz	-31.5	403 MHz	-34
	433 MHz	-29.2	433 MHz	-31.7
	2.45 GHz	-26.3	2.45 GHz	-27.64
The reflection coefficient S_{11} (dB)	403 MHz	-13.482	403 MHz	-8.781
	433 MHz	-13.45	433 MHz	-8.9
	2.45 GHz	-10.97	2.45 GHz	-5.443
The maximum SAR (rms,1g)	403 MHz	224.596	403 MHz	345.896
	433 MHz	210.713	433 MHz	334.228
	2.45 GHz	201	2.45 GHz	214.231

IV. EVALUATION IN AN ANATOMICAL ARM MODEL

The proposed antenna is designed and evaluated first in the simplified body model as shown in previous sections. However, it should be also evaluated in the anatomical body model that provides a better resemblance of the real human body than the simplified body model. Indeed, the anatomical body model is considered as the best tool for evaluating the performance of implantable antennas [28]. Therefore, the proposed antenna is simulated in the left arm of the CST Katja voxel body model. The CST Katja voxel body model represents a 43-year old female with a height of 163 cm and weight of 62 kg [29]. The anatomical arm model of implantation is shown in Fig. 17. The exact position of implantation in the muscle layer inside

this model is also shown in the same figure. The antenna is proposed for glucose monitoring applications. Hence, it is simulated at this position of implantation [1].

The reflection coefficient S_{11} (dB) is shown in Fig. 18. It can be seen from the figure that the resonant frequency has been shifted down by around 25 MHz inside the arm of the CST Katja voxel body model in comparison with that in the simplified body model. However, the -10 dB matching is still obtained for all of the intended bands of operation as the antenna is broad in bandwidth.

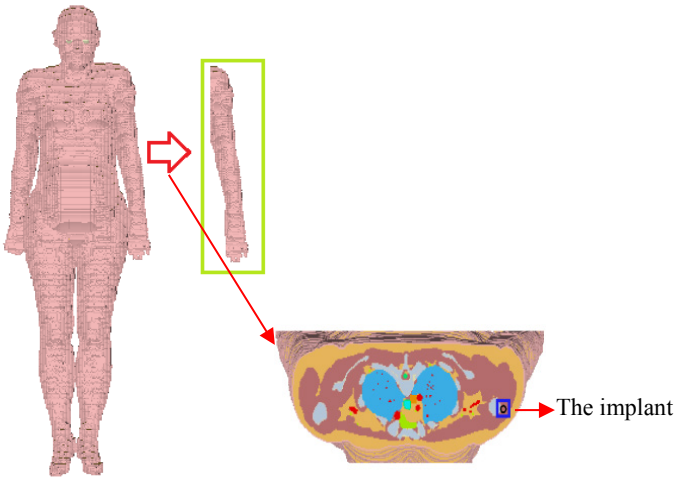

Fig. 17. The anatomical body model of evaluation

The antenna gain and radiation efficiency are decreased by 2 dB. The anatomical body model is multilayer unlike the simplified body model. Hence, extra reflection losses between the skin-fat, fat-muscle and muscle-bone are obtained inside of it. However, the gain value is relatively large for this small implant size. It is also good enough to build up a wireless communication link over 2 m [1], [11].

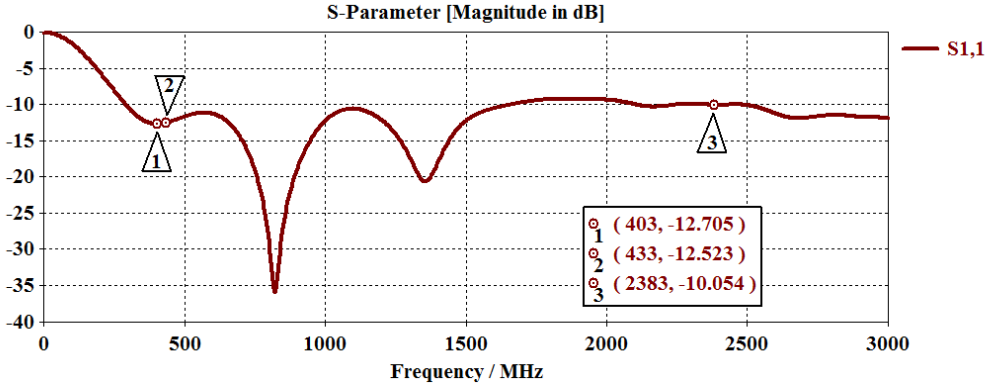

Fig. 18. The reflection coefficient S11 (dB) of the proposed cloud shape loop antenna in the arm of the CST Katja voxel body model

The performance of the proposed antenna is compared with that for other conformal and flexible designs proposed recently in literature as summarized in Table 3. Although some flexible antennas work for the same three bands such as in [6] and [18], these antennas are used with implants of larger sizes than those of the implant with which the proposed cloud loop antenna can be used. Implants in general are preferred to be small in size. When the implant size increases, the overall losses around the antenna become smaller as the implant replaces the lossy area around the antenna. This causes a larger radiation efficiency and gain.

TABLE 3
SUMMARY OF THE MAIN CHARACTERISTICS OF SOME RECENT CONFORMAL AND FLEXIBLE IMPLANTABLE ANTENNAS PROPOSED IN LITERATURE

Ref.	Freq. Bands	Radiation Efficiency, dB	Gain, dBi	Body Model Shape and Maximum Dimensions, mm	Implant Size, mm^3	Complexity	Application
[6]	401-406 MHz	-29.2 at 403 MHz	-26	elliptical (180,100, 50)	$\pi\times(5)^2\times15$	complex	glucose monitoring of adults
	433-434 MHz	-27 at 433 MHz	-25.1				
	2.4-2.5 GHz	-22.8 at 2.45 GHz	-15				
[11]	401-406 MHz	-32.4 at 403 MHz	-28.8	cylindrical (80, 110)	$\pi\times(5)^2\times32$	complex	glucose monitoring of adults
	2.4-2.5 GHz	-22.76 at 2.45 GHz	-18.5				
[14]	401-406 MHz	-31.3 at 403 MHz	-28.4	elliptical (180,100 ,50)	$\pi\times(3.2)^2\times10$	simple	capsules for kids
	433-434 MHz	-------	--------				
[15]	401-406 MHz	-------- at 403 MHz	-28.95	cylindrical (120,110)	$\pi\times(5)^2\times15$	simple	glucose monitoring of adults
	433-434 MHz	--------	--------				
[16]	401-406 MHz	-33 at 403 MHz	-27.6	cylindrical (80, 100)	$\pi\times(5)^2\times40$	simple	bone implants
	433-434 MHz	---------	--------				
[17]	2.4-2.5 GHz	-28.54 at 2.45 GHz	-23.98	rectangular (180,60,60)	≈4.12×25.5	simple	general implantable applications (no specific application is provided)
[18]	401-406 MHz	-37.7 at 403 MHz	-34.36	rectangular (355,266, 160)	$(\pi\times(16)^3)/3$	simple	implanted central venous catheters (CVC)
	433-434 MHz	----------	---------				
	2.4-2.5 GHz	-32.3 at 2.45 GHz	-26.14				
Cloud This work	401-406 MHz	-36.2 at 403 MHz	-31.5	cylindrical 100×50	$\pi\times(3.7)^2\times10.6$	simple	glucose monitoring
	433-434 MHz	-33.67 at 433 MHz	-29.2				
	2.4-2.5 GHz	-30.2 at 2.45 GHz	-26.3				

Moreover, the design in [6] is a bit complicated as small complementary split rings were integrated to its structure. Some of these antennas obtained larger radiation efficiency and gain than the proposed antenna such as in [11], [15] and [17]. However, they work for only one or two bands. Although the antenna in [14] has a smaller size than the proposed antenna, it works for the 401-406 MHz MedRadio and 433-434 MHz ISM bands only. When the antenna becomes broader in bandwidth such as the antenna proposed in this work, radiation efficiency and gain are decreased. Despite this, the proposed cloud loop antenna has obtained 1 dB larger radiation efficiency and gain than the design in [14] when simulated in the same body model. In summary, the cloud loop antenna proposed in this work has satisfied many challenging requirements for implantable applications that have not been satisfied simultaneously for other designs proposed in literature; it consists of a simple structure, a broad bandwidth, relatively large radiation efficiency and gain, and work for all bands required to transfer and save power for implantable applications. This antenna can also work for small implants. The antenna proposed in this paper is the smallest flexible antenna that can work for all of the 401-406 MHz MedRadio, 433-434 MHz and 2.4-2.5 GHz ISM bands at the same time.

V. CONCLUSIONS

In this paper, a broadband flexible loop antenna is proposed for muscle implantable devices. The antenna has a broad bandwidth that covers the 401-406 MHz MedRadio and the 433-434 MHz and 2.4-2.5 GHz ISM bands. This supports the functionalities of data transmission, wireless power transfer and power saving. The antenna has a very simple structure exploited carefully to increase the total power radiated from the antenna. This has been indicated by comparing radiation efficiency and gain of the proposed antenna with those of a typical elliptic cylindrical loop antenna. The proposed antenna has a larger radiation efficiency and gain than those for the typical elliptic cylindrical loop antenna of comparison. The antenna performance is evaluated in simple and anatomical body models; and a robust performance has been always obtained.

REFERENCES

[1] R. Alrawashdeh, *Implantable Antennas for Biomedical Applications*, Ph.D. dissertation, University of Liverpool, Liverpool, U.K., 2015.

[2] A. Vorst, A. Rosen, and Y. Kotsuka, *RF/Microwave Interaction with Biological Tissues*, Hoboken, New Jersey: John Wiley & Sons Ltd, 2006.

[3] Electromagnetic Compatibility and Radio Spectrum Matters (ERM); Short Range Devices (SRD); Ultra Low Power Active Medical Implants (ULP-AMI) and Peripherals (ULP-AMI-P) operating in the frequency range 402 MHz to 405 MHz; Part 1 and Part 2, European Telecommunications Standards Institute (ETSI) Std. EN 301 839-1/2 V1.3.1, 2007. [Online]. Available: www.etsi.org

[4] IEEE Standard for Safety Levels with Respect to Human Exposure to Radio Frequency Electromagnetic Fields, 3 kHz to 300 GHz, IEEE Standard C95.1-1999, 1999.

[5] IEEE Standard for Safety Levels with Respect to Human Exposure to Radio Frequency Electromagnetic Fields, 3 kHz to 300 GHz, IEEE Standard C95.1-2005, 2005.

[6] R. Alrawashdeh, Y. Huang, M. Kod, and A. Sajak, "A Broadband flexible implantable loop antenna with complementary split ring resonators," *IEEE Antennas and Wireless Propagation Letters*, vol. 14, pp. 1506-1509, 2015.

[7] Z. Yang, S. Xiao, L. Zhu, B. Wang, and H. Tu, "A circularly polarized implantable antenna for 2.4-GHz ISM band biomedical applications," *IEEE Antennas and Wireless Propagation Letters*, vol. 16, pp. 2554-2557, 2017.

[8] M. Fazeli, *Implantable Ferrite Antenna for Biomedical Applications*, M.Sc. thesis, Tuscaloosa, Alabama, USA, 2016.

[9] P. Loktongbam and L. Solanki, "Design and analysis of an implantable patch antenna for biomedical applications," *International Journal of Engineering Technology Science and Research*, vol. 4, no.5, pp. 126-138, 2017.

[10] S. Dinesh, R. Priyan, and R. Jothichitra,"Design of implantable patch antenna for biomedical application," *Proceedings of International Conference on Innovations in Information, Embedded and Communication Systems*, pp. 1-6, 2015.

[11] F. Merli, *Implantable Antennas for Biomedical Applications*, Ph.D. dissertation, EPFL University, Lausanne, Switzerland, 2011.

[12] X. Li, M. Jalilvand, W. You, W. Wiesbeck, and T. Zwick, "An implantable stripline-fed slot antenna for biomedical applications," *Proceedings of IET International Radar Conference*, pp. 1-5, 2013.

[13] J. Samuel and C. Jaison, "Miniaturized loop antenna for implantable medical device," *Proceedings of International Conference on Emerging Technological Trends*, pp. 1-5, 2016.

[14] R. Alrawashdeh, Y. Huang, and P. Cao, “Flexible meandered loop antenna for implants in the MedRadio and ISM bands,” *Electronics Letters*, vol. 49, no. 24, pp. 1515-1517, 2013.

[15] R. Alrawashdeh, Y. Huang, and P. Cao, "A conformal U-shaped loop antenna for biomedical applications," *Proceedings of European Conference on Antennas and Propagation*, pp. 157-160, 2013.

[16] R. Alrawashdeh, Y. Huang, and A. Sajak, "A flexible loop antenna for biomedical bone implants," *Proceedings of European Conference on Antennas and Propagation*, pp. 861-864, 2014.

[17] M. Scarpello, D. Kurup, H. Rogier, D. Ginste, F. Axisa, J. Vanfleteren, W. Joseph, L. Martens, and G. Vermeeren, "Design of an implantable slot dipole conformal flexible antenna for biomedical applications," *IEEE Transactions on Antennas and Propagation*, vol. 59, no. 10, pp. 3556-3564, 2011.

[18] C. Schmidt, F. Casado, A. Arriola, I. Ortego, P. Bradely, and D. Valderas, "Broadband UHF implanted 3-D conformal antenna design and characterization for in-off body wireless links," *IEEE Transactions on Antennas and Propagation*, vol. 62, no. 3, pp. 1433-1444, 2014.

[19] R. Elyassi and G. Moradi, "Flexible and moon-Shaped slot UWB implantable antenna design for head implants," *International Journal of Microwave and Wireless Technologies*, vol. 9, no. 8, pp. 1559-1567, 2017.

[20] A. Ibraheem and M. Manteghi, "Performance of an implanted electrically coupled loop antenna inside human body," *Progress In Electromagnetics Research*, vol. 145, pp. 195-202, 2014.

[21] A. Sharma, E. Kampianakis, and M. Reynolds, "A dual-band HF and UHF antenna system for implanted neural recording and stimulation devices," *IEEE Antennas and Wireless Propagation Letters*, vol. 16, pp. 493-496, 2017.

[22] Y. Huang and K. Boyle, *Antennas from Theory to Practice*, UK, Chichester: John Wiley & Sons Ltd, 2008.

[23] R. Moore, "Effects of a surrounding conducting medium on antenna analysis," *IEEE Transactions on Antennas and Propagation*, vol. 11, no. 3, pp. 216-225, May 1963.

[24] D. Andreuccetti, R. Fossi, and C. Petrucci, "Calculation of the dielectric properties of body tissues in the frequency range 10 Hz-100 GHz," Institute for Applied Physics, Italian National Research Council, Florence (Italy), 1997. Accessed: Jan. 25, 2019. [Online]. Available: http://niremf.ifac.cnr.it/tissprop/

[25] CST- Computer Simulation Technology. (2013). Accessed: Jan. 25, 2019. [Online]. Available: http://www.CST.com

[26] A. Rodrigues, L. Malta, R. Borsali, R. Takai, R. Conhalato, L. Rodrigues, J.A. Vasconcelos, T. Green, and J. Ramirez, "SAR calculations in an anatomically realistic model of the head of cellular phone users," *Proceedings of The Fourth International Conference on Computation in Electromagnetics*, pp. 1-2, 2002.

[27] M. Asili, R. Green, S. Seran, and E. Topsakal, "A small implantable antenna for MedRadio and ISM Bands," *IEEE Antennas and Wireless Propagation Letters*, vol. 11, pp. 1683-1685, 2013.

[28] R. Alrawashdeh, Y. Huang, and Q. Xu, "Evaluation of implantable antennas in anatomical body models," CST article, 2014. [Online]. Available: https://www.cst.com/solutions/article /evaluation-of-implantable-antennas-in-anatomical-body-models.

[29] CST Studio Suite, BioEM Simulation Using CST STUDIO SUITE 2013. Accessed: Jan. 25, 2019. [Online] Available: https://www.cst.com/-/media/cst/events/user-conferences/ documents/2013/session-5-4/5-4-2_cst_euc.ashx?la=en&hash=C559E23426F8E7E7C5207CF CAD9625537CAB0FF3.